Available free online at www.medjchem.com

Mediterranean Journal of Chemistry

Mediterranean Journal of Chemistry **2019**, 8(4), 328-337

Effect of bismuth and bore content in glass system inhibitor on the corrosion behavior of mild steel in 1M hydrochloric acid solution

Azeddine Elbadaoui[1], Mouhsine Galai [2,*], Soumya Ferraa[1], Hanane Barebita[1], Mohammed Cherkaoui [1] and Taoufiq Guedira [1]

[1] Laboratory of Materials, Electrochemistry and Environment, Faculty of Science, Ibn Tofail University, BP. 133-14000, Kénitra, Morocco

[2] Laboratory of Materials Engineering and Environment: Modeling and Application, Faculty of Science, Ibn Tofail University, BP. 133-14000, Kenitra, Morocco

Abstract : The influence of (0.90-x) Bi_2O_3-xB_2O_3-0.10 (Ta_2O_5-Nb_2O_5) on the corrosion behavior of mild steel in 1M hydrochloric acid was studied. Electrochemical polarization and impedance spectroscopic methods measurements were used. The inhibition efficiency increases with S1 concentration to reach 79% at 150 ppm. Polarization curves show that our inhibitors. S1 is a cathodic inhibitor type. The increase in temperature leads to a decrease in the inhibition efficiency of the used inhibitor. The thermodynamic study showed that the film was formed at the steel surface by physisorption in the presence of inhibitor. Moreover, in this study, the results showed that the inhibition efficiencies depend on the B_2O_3 and Bi_2O_3 content in the glass. it is observed that the value at 50% of B_2O_3 in the glass provided better protection than the other content.

Keywords: Glass; corrosion inhibitor; mild Steel; 1.0 M Hydrochloric acid.

Introduction

The corrosion results from chemical or electrochemical action of an environment on the metals and alloys. The consequences are significant in various fields and in particular in the industry: production stoppage, replacement of corroded parts, accidents and risks of pollution are frequent events with sometimes substantial economic consequences [1].

In terms of protection, corrosion inhibitors are a necessary means of protection against metal corrosion. An inhibitor is a chemical compound that is added in a small concentration to the medium to minimize the corrosion rate of the materials [2-8].

The use of corrosion inhibitors is the best economical method to minimize mild steel corrosion. Heterocyclic compounds containing heteroatoms such as N, S and Oxygen present a suitable inhibitor to stop la corrosion for mild steel in various acid medium, and many publications use these compounds [9-12].

For many industries that do the treatment of cooling, water circuits use different formulations to protect the pipes against corrosion. The majority of inhibitors used in these mediums are inorganic compounds [13-16].

The objective of this study is to investigate the influence of inhibitor (glass) addition on the corrosion of mild steel in acidic medium 1.0 M HCl.

Experimental

Synthesis of the vitreous phases of the system Bi_2O_3-B_2O_3-(Ta_2O_5-Nb_2O_5)

The vitreous phases of the system Bi2O3-B2O3-(Ta2O5-Nb2O5) are obtained by fusion of the stoichiometric mixtures of the starting products according to the reaction pathway:
(1-x-y)Bi2O3+xB2O3+y/2Ta2O5 + y/2Nb2O5 (1-x-y) Bi2O3+xB2O3+ y/2Ta2O5 + y/2Nb2O5.

The reagents carefully are crushed in an agate mortar then introduced into alumina crucibles.
First heat treatment was carried out at 350°C during one night followed by crushing; the temperature was increased by 50 °C in order to avoid the chemical losses by volatilization; followed by melting at 950°C.

The reactional mixture is then brought up to a higher temperature at the melting point. The molten mixture is then soaked with the free air in a mould out of alumina heated beforehand with approximately 200°C.

*Corresponding author: Mouhsine Galai
Email address: galaimouhsine@gmail.com
DOI: http://dx.doi.org/10.13171/mjc841907012mg

Received February 16, 2019
Accepted April 11, 2019
Published July 1, 2019

The band between 1190-1240 cm^{-1} is allotted to the vibration of the final groupings B-O- in units pyroborates [17-19].

On the other hand, the line around 1270-1310 cm^{-1} is allotted to the asymmetrical mode of elongation B-O in the unit's orthoborate (BO_3).

The progressive addition of B_2O_3 causes an increase in the intensity of the bands located towards 420-490, 500-540,600-690 cm^{-1} and the reduction in the intensity of the band around 1190-1240 cm^{-1}. The wide strip located around 980-1000 cm^{-1} is dominant.

Reduction in the intensity of line around 1190-1240 cm^{-1} assigned with the units pyroborates compared to that located towards 600 - 690 cm^{-1} relative with the métaborates are explained by the conversion of the units pyroborates into units métaborates.

However, the reduction in the intensity of the band allotted to the pyroborates compared to the full strip towards980-1000 cm^{-1} seems related to the conversion of the pyroborates into entities diborate. This transformation is probably related to the increase in the rate of boron atoms in co-ordination number IV.

The band between 640-650 cm^{-1} corresponds to the vibration of connection Ta-O, and the band 870 cm^{-1} is allotted to the vibration of the connection Ta-O-Ta [20].

In general, the band from 600 to 950 cm^{-1} of Nb-O vibrations of elongation can be observed [21]. The close band IR 920 cm^{-1} is allotted to the mode of stretching of connections Nb- O while strongest nearly 620 cm^{-1} was allotted to the stretching of more than bridging connections Nb-O-Nb deformed in NbO6 octahedral [22]. In particular, in the area from 500 to 700 cm^{-1} area of vibrations of the valence of Ta-O-Nb.

Studies of glasses of compositions (0.90-x) Bi_2O_3-x B_2O_3-0.10 (Ta_2O_5-Nb_2O_5)

Table 1 gives the molar fractions corresponds to the compositions (0.90-x) Bi2O3-xB2O3 0.10(Ta2O5-Nb2O5). Figure 1 represents the infra-red spectra of these compositions. The frequencies and their attributions are consigned in Table 2.

Table1. Composition of the samples prepared within the system (0.90-x) Bi_2O_3-xB_2O_3-0.10 (Ta_2O_5-Nb_2O_5).

sample.N°	**0.95-x**	**x**
S_1	0.65	0.3
S_2	0.6	0.35
S_3	0.55	0.4
S_4	0.5	0.45
S_5	0.45	0.5

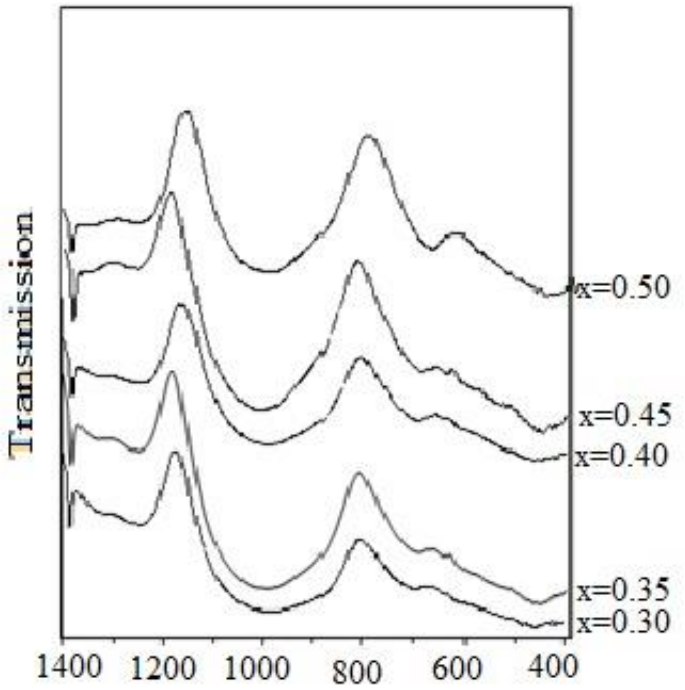

Figure 1. Spectra infra-red of glasses of compositions (0.90-x)Bi_2O_3-xB_2O_3-0.10 (Ta_2O_5- Nb_2O_5).

The analysis of the infra-red spectra of glasses of composition (0.90-x) Bi2O3-x B2O3-0.1(Ta2O5Nb2O5) shows that the substitution of bismuth by boron involves an increase in the intensities of the bands assigned with the units méthaborates B-O-Bi and Bi-O Bi. We also observe the disappearance of the inversion of υas (BO) inBO3. We also notice a disappearance of the groupings orthoborates BO3. This can be explained by the conversion of the units orthoborates into unit métaborates.

The increase in the content of Ta2O5 and Nb2O5 in the system Bi2O3-B2O3- (Ta2O5-Nb2O5) involves

- A disappearance of the band corresponding to the groupings orthoborates BO_3.

- A disappearance of the inversion of υas (BO) in BO_3.

Table 2. Attributions of the infra-red frequencies of glasses of compositions (0.90-x) Bi2O3-x B2O3-0.10(Ta2O5-Nb2O5).

N° de l'échantillon		**S_1**	**S_2**	**S_3**	**S_4**	**S_5**
Composition		x=0.30	x=0.35	x=0.4	x=0.45	x=0.5
Attributions	υ squelette (Bi-O-Bi) υ squelette (B-O-Bi)	426 457	426 462	430 462	448 462	471 490
	υ squelette (B-O-B)	----	529	540	548	548
	υ (Nb-O)	----	558	563	581	----
	υ (Ta-O-Nb)	666	687	668	681	687
	υ (Nb-O-Nb)	609	610	613	613	613
	υ (Ta-O)	633	634	635	641	660
	boroxol	885	890	891	900	900
	orthoborates BO_3	-----	----	----	----	----
	υ_s BO (BO^{4-})	982	992	1004	1006	1010
	Pyroborates B-O^-	1244	1250	1250	1250	1260
	υ_{as}(BO) dans BO_3	1319	---	---	---	---

Electrochemical measurements

Before each experiment, the mild steel ((wt.%) C = 0.21, Mn = 0.05, Si = 0.38, S = 0.05, P = 0.09, Al = 0.01 and the remaining iron) was polished using emery paper until 1200 grade. After this, it was decreased with ethanol, rinsed with distilled water and finally dried at room temperature. The aggressive solution (1 M HCl) was prepared by dilution of Analytical Grade 37% HCl with distilled water. Inhibitors corrosion (Table 1) were added at their powder form to acid solution in the range of 100-300 ppm concentrations.

The potentiodynamic polarization curves were recorded by scanning the electrode equilibrium potential automatically from E_{corr} to the negative values and from E_{corr} to the positive values by using a potentiostat / Galvanostat PGZ 100 with scan rate equal 1 mV/S after 0.5 h of immersion in order to reach the state of equilibrium. The temperature of the solution was 298 K. The electrochemical cell used had three electrodes. The reference electrode was a saturated calomel electrode (SCE). A platinum electrode was used as an auxiliary electrode. The working electrode was mild steel.

The extrapolation of Tafel lines calculates the electrochemical parameters. The effectiveness of corrosion inhibition is evaluated from values of corrosion current densities using relation (3):

$$\eta_{PP} = \frac{i^0_{corr} - i_{corr}}{i^0_{corr}} \times 100$$

Where i^0_{corr} and i_{corr} are the values of corrosion current densities without and with inhibitor, respectively.

The electrochemical impedance spectroscopy was performed using a transfer function of the analyzer (VoltaLab PGZ100), with a low signal

amplitude (10 mV rms), over a frequency range from 100 KHz to 100 MHz with ten points per decade. The SIE diagrams were carried out in the representation of Nyquist. The results were then analyzed via an equivalent electrical circuit using the Brockamp program [23].

The inhibition efficiency from the SIE is also calculated using the following equation:

$$\eta_{EIS} = \frac{R_{ct} - R_{ct}^{0}}{R_{ct}} \times 100$$

Where R_{ct}^{0} and R_{ct} are the values of the charge transfer resistance in the absence and the presence of the inhibitor, respectively.

Results and Discussion

Electrochemical Impedance Spectroscopy

The corrosion study of mild steel in 1M HCl solution with and without inhibitor was investigated by electrochemical impedance spectroscopy. The Nyquist representations of the behavior of mild steel in 1M HCl with the addition of the various concentrations of S1 are presented in Figure 2.

From this Figure, all concentration of S1 does not have perfect semicircles due to the frequency dispersion. The loop diameter increased when the inhibitor concentration increase. The size of the highest loop is attributed to the adsorption of the inhibitor molecule [24].

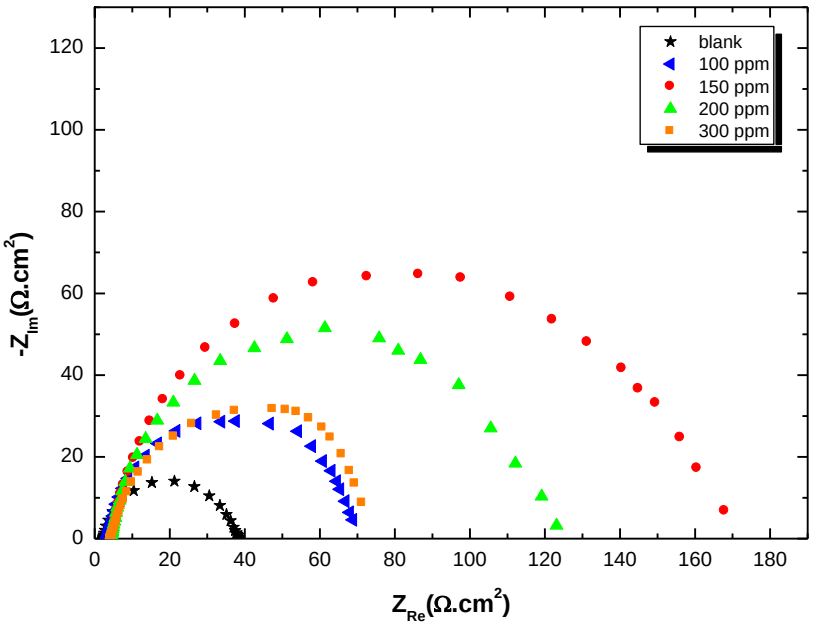

Figure 2. Nyquist diagrams obtained for mild steel in 1M HCl that contain the different S1 concentrations after 30 min of immersion.

Table 3. Electrochemical impedance parameters in HCl 1 mol/L at different S1 concentration.

Cinh (M) of S1	Rct(ohm.cm²)	Cdl(µf/cm²)	E%
Blank	35	284	-
100ppm	69	274	49
150ppm	168	124	79
200ppm	122	285	71
300ppm	73	261	52

From Table 3, the values of Rt become more extensive with the decrease of the concentration of S1 and which holds a higher value at150 ppm, which means a reduction in the rate of corrosion. The inhibitory efficacy E (%), of this inhibitor, evolves in the same way as Rt and achieves a better inhibitory efficiency is 79 %.

The addition of the glass S1 decreases the value of the double-layer capacitance Cdl and passes from 284 µF.cm^{-2} for the white to 124 µF.cm^{-2}. The decrease of the Cdl value can be attributed to the adsorption of the ions composition of the inhibitor on the surface of the steel [25-27], in fact, more inhibitor adsorbs, the thickness of the film of the inhibitor increases and the double layer capacity decreases.

Polarization curves

The cathodic and anodic polarization curves of the working electrode in 1M HCl in the absence and presence of various concentrations of S1 after pre-polarization of the mild steel at its E_{corr} for 30 minutes are presented in Figure 3. The different

electrochemical parameters extracted from these polarization curves, the corrosion current density (icorr), the corrosion potential (Ecorr), the cathodic Tafel slope (βc) are associated in Table 4. Also, the cathodic Tafel slopes (βc) calculated from Figure 3 is unchanged when the concentration of inhibitor increase. This observation shows that the activation controls hydrogen evolution, and the presence of inhibitor does not change the mechanism of the cathodic evolution reaction [28-29].

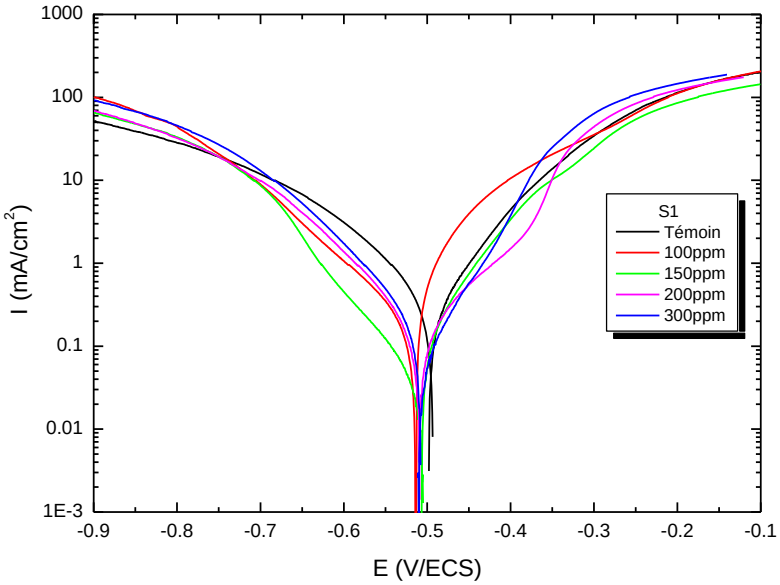

Figure 3. Polarization curves of the working electrode (mild steel) in 1M hydrochloric acid obtained at 25 ° C with the addition of the inhibitor at various concentrations of S1

Table 4. Potentiodynamic polarization parameters for the working electrode (mild steel) in 1M hydrochloric acid obtained at 25 ° C with the addition of the inhibitor at various concentrations of S1.

S1	E_{corr}(mV/ECS)	i_{corr}(µA/cm²)	βc (mv)	E%
Blank	-497	983	-92	-
100ppm	-507	474	-83	51
150ppm	-503	201	-87	79.5
200ppm	-512	281	-100	71
300ppm	-506	456	-86	54

From Table 4, the inhibition efficiency increased with decreasing the concentration of S1 and this inhibitor affect the cathodic and anodic inhibition through adsorption on the working electrode surface by blockage of the active sites [30]. The corrosion potential Change slightly. According to Riggs et al. [31] if the displacement in the potential of corrosion (i) is >85mV, the inhibitor acts as a cathodic or anodic type, (ii) if the displacement is <85, the inhibitor acts as mixed type. Effectively in our case, the displacement is lower than 85, which can have classified our inhibitor S1 as a mixed type. Table 4 shows that the inhibition efficiency E% increases when the concentration of the S1 decrease also i_{corr} decreases with when the concentration of S1 decrease. The higher inhibition efficiency is 79.5 %, and it obtained at 150 ppm of S1 in 1M HCl.

Effect of temperature

Potentiodynamic polarization measurements

The influence of temperature on the inhibition of inhibitors, particularly the acidic environment, has been the subject of several articles; During pickling and descaling at high temperature, and in order to get rid of the corrosion products on the metallic installations, the inhibitors have the role of protecting the latter against acid attacks. Figures 4 and 5 show the polarization curves in 1M HCl in the absence and the presence of S1 for the concentration of 150 ppm. The choice of concentration 150 ppm is justified by the fact that at this concentration, the value of the efficiency is maximum.

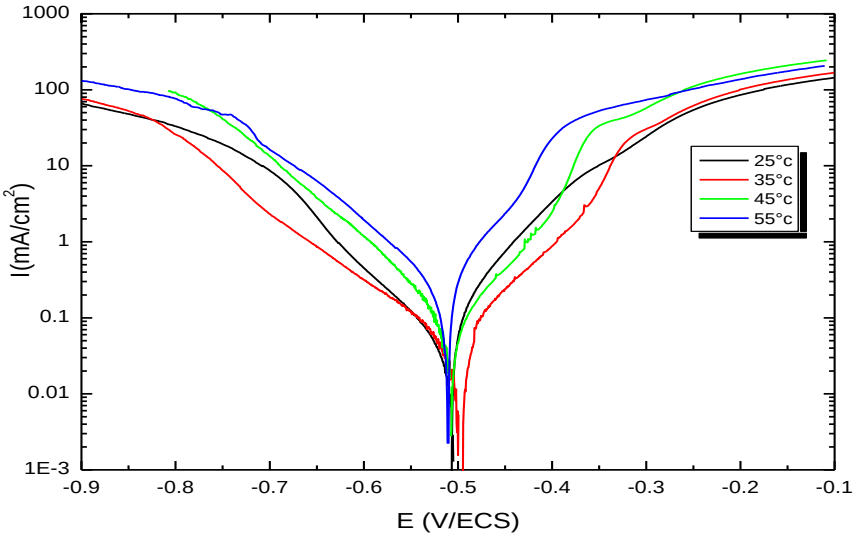

Figure 4. Polarization curves obtained for a working electrode in 1M of hydrochloric acid solution at different temperatures in the presence of 150 ppm of S1.

Table 5. The electrochemical parameters for working electrode in 1M of a hydrochloric acid solution containing 150 ppm of S1 at various temperature.

	E_{corr}(mV/ECS)	i_{corr}(µA/cm²)	βc (mv)	E%
25C°	-503	201	-87	79.5
35 C°	-491	368	-82	77
45 C°	-509	577	-76	76
55 C°	-511	752	-83	75

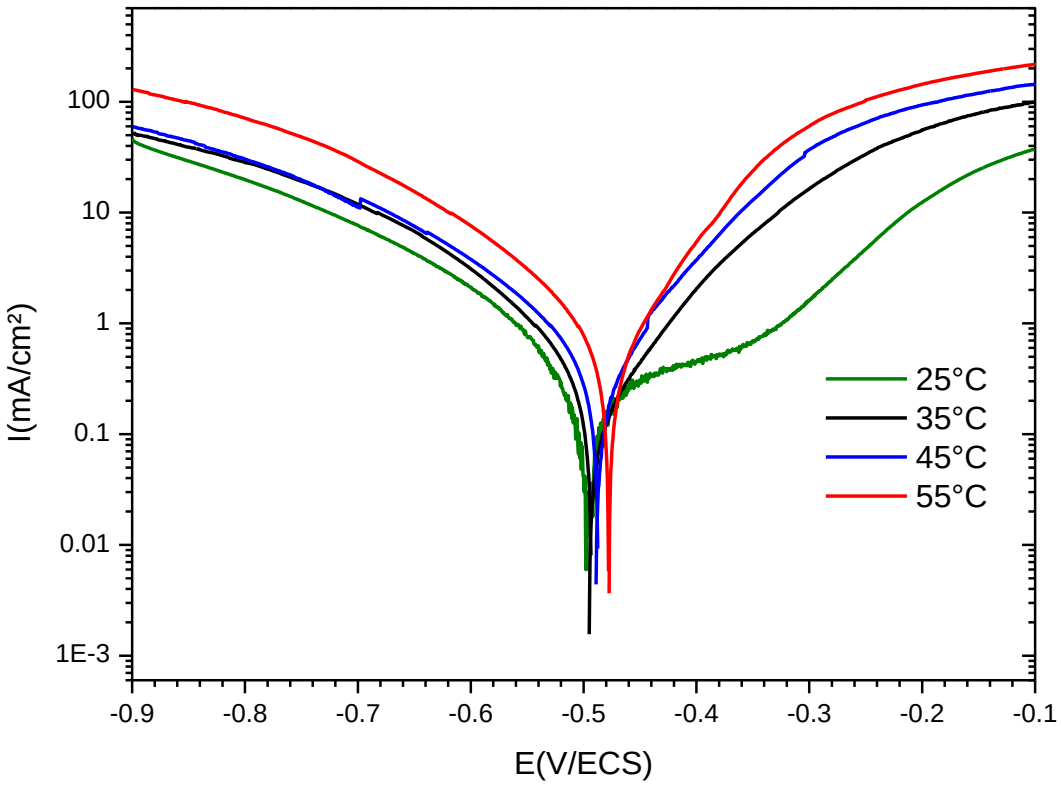

Figure 5. Potentiodynamic polarization curves for working electrode in 1M of hydrochloric acid solution at various temperatures.

Table 6. the electrochemical parameters for working electrode in 1M of hydrochloric acid solution (Blank solution).

	E_{corr} (mV/ECS)	i_{corr} (µA/cm²)	βc (mv)
25C°	-497	983	-92
35 C°	-491	1600	-184
45 C°	-475	2420	-171
55 C°	-465	3100	-161

From Table 6, the S1 inhibitor efficiencies are depended on the temperature. Also, the inhibitor efficiencies decrease with temperature; this observation can be attributed to the specific interaction between the Fe substrate surface and the inhibitor [32].

Thermodynamic part

For more details on the corrosion process, activation kinetic parameters such as activation energy (Ea), enthalpy (ΔH*) and entropy ΔS*) were evaluated according to the Arrhenius law and the alternative formula of the following Arrhenius equation [33]:

$$i_{corr} = K \exp(\frac{-E_a}{RT})$$

Where:
Ea: activation energy,
K: pre-exponential factor,
R: the universal gas constant
T: the absolute temperature presented in K

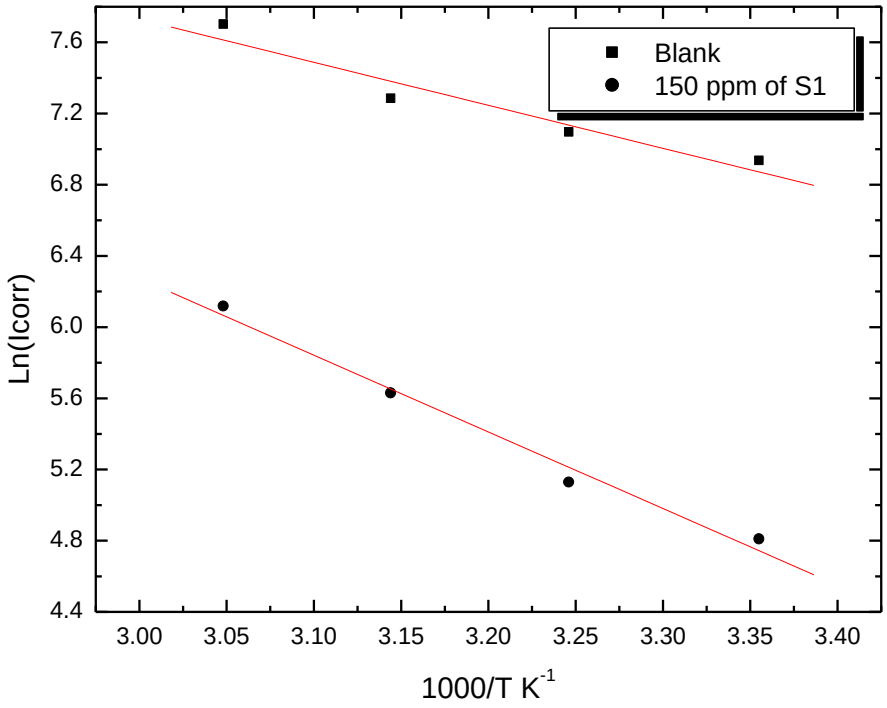

Figure 6. Arrhenius strains calculated from i_{corr} of the working electrode in 1M hydrochloric acid and for 150 ppm of S1.

The linear regression coefficients are close to the unit, indicating that the mild steel corrosion in HCl 1M can be calculated by using the Arrhenius model. From Table 7, the Ea of 150 ppm of S1 was higher than that of Blank solution. This increasing in Ea can interpret as physical adsorption. Effectively, a higher energy barrier for the corrosion process in the solution containing the inhibitor is involved with physical adsorption or weak chemical bonding between the compound molecule and the substrate surface [34]. Szauer et al. demonstrate that the higher value of Ea can be explained to a decrease in the adsorption processes of the inhibitor (glass) on the substrate surface when the temperature increase [35].

The formula of the Arrhenius equation allows the determination of enthalpy and entropy according to the next equation:

$$Icorr = \frac{k_B\ T}{h} \exp\left(\frac{\Delta S^*}{R\ T}\right) exp\left(\frac{-\Delta H^*}{R\ T}\right)$$

Where:
h: Planck's constant,
K_B:is Boltzmann constant,
R: the universal gas constant,
ΔH^*_a: the enthalpy of the activation
ΔS^*_a: the entropy of activation.

Figure 7 illustrates the variation of ln icorr / T as a function of the inverse of the temperature for the acid solution and the concentration of 150 ppm of S1. The straight lines obtained have a slope equal to (-ΔH * / R) and an ordinate at the origin equal to (ln (R / Nh) + ΔS * / R). ΔH * and ΔS *. The values of enthalpies ΔH * and entropies and ΔS * are given in Table 7.

From Table 7, the ΔHa* values for dissolution reaction of mild steel in 1.0 M HCl in the presence of 150 ppm of S1 is higher than the blank solution (28 kJ mol^{-1}). The positive signs of ΔHa* values reflect the endothermic nature of the Fe substrate dissolution mechanism; this dissolution is slow [36]. Also, the values of Ea is higher than the s value of ΔHa* indicating that the corrosion must be associated to a gaseous reaction, the hydrogen evolution reaction, involved with a decrease in the total reaction volume [37].

Also, the Table 7 shows that the ΔS* value increase in the presence of inhibitor compared to the uninhibited solution, which means an increase in disorder occurs during the transition from reactant to the activated complex during the corrosion mechanism [38-39].

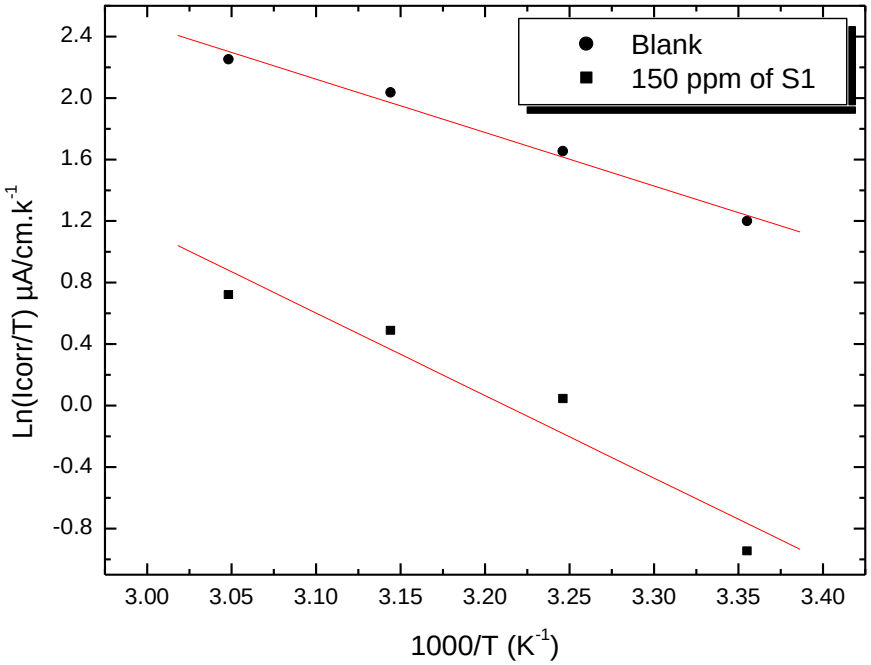

Figure 7. Transition Arrhenius plots for mild steel in 1M hydrochloric solution in the absence and the presence of 150 ppm of S1.

Table 7. Activation parameters for working electrode corrosion in 1M of the hydrochloric solution in the absence and the presence of 150 ppm of S1.

	EA KJ/mol	**ΔH KJ/mol**	**ΔS KJ/mol**
Blank	31.5	28	-107
150 ppm S1	36	33.3	-50

Effect of Bore content in the glass

The corrosion behavior of mild steel in 1M of hydrochloric solution for different compositions of glasses in the system (0.95-x) Bi2O3-x B2O3-0.05at 150 ppm, was investigated using EIS method at 25°C after 0.5 h of immersion at corrosion potential (Fig. 8). The effect of bore (B) and bismuth (Bi) on the corrosion resistance of mild steel in 1 M HCl solution was investigated. in other studies, the presence of both increase the resistance of transfer of charge Rct according to [40].in this study we are increasing the concentration of bore and bismuth comparing with former study, moreover the percentage of Ta and Nb are also increasing in these glasses systems.

It is noticed from these plots presented in Figure 8 that the impedance of mild steel in uninhibited solution (Blank solution) has changed after the addition of each inhibitor. The higher is obtained when the glass contains a high content of B_2O3. The electrochemical parameters and the inhibition efficiencies values are regrouped in Table 8 for all percentage of B_2O_3, the addition of glasses in the blank solution the charge transfer resistance increase. This change can be attributed to the decrease in the local dielectric constant, and an increase in the thickness of the electrical double layer suggests that the glasses molecules by adsorption at the metal/solution interface [41].

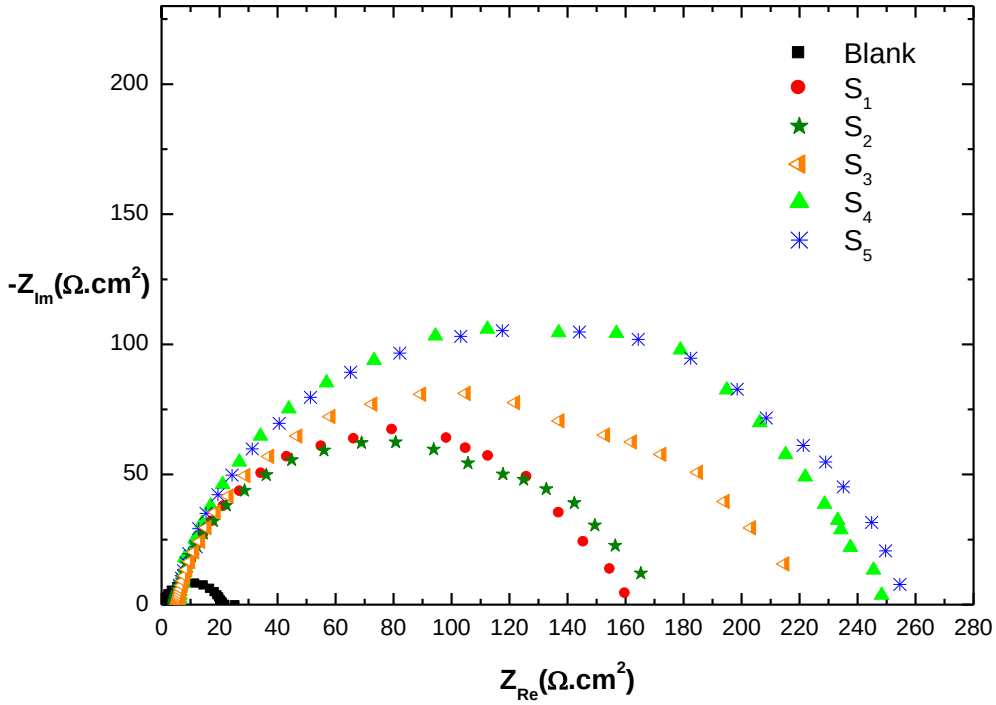

Figure 8. Impedance diagram of working electrode recoded in 1 M HCl containing 150 ppm of each (0.90-x) Bi_2O_3-x B_2O_3-0.10-(Ta_2O_5-Nb_2O_5) at corrosion potential (x varied from 0.3% to 0.5%).

Table 8. Electrochemical parameters obtained from the Nyquist plots representation for mild steel in 1M HCl containing 150 ppm of (0.90-x) Bi_2O_3-x B_2O_3-0.10-(Ta_2O_5-Nb_2O_5). glass system (x varied from 0.3% to 0.5%).

Cinh (M) of BA6	Rct(ohm.cm²)	Cdl(µf/cm²)	E%
blank	35	284	-
s1	168	124	79
s2	170	111	79.5
s3	222	105	84
s4	251	99	86
s5	258	84	86.5

The inhibition efficiency increases with B_2O_3content and reaching a higher value at 50% of B_2O_3. The adsorption of these products on mild steel displaces the water molecule and other ions already adsorbed [42].

Conclusion

The glasses (0.90-x) Bi2O3-x B2O3-0.10(Ta2O5-Nb2O5) system were prepared and then characterized by X-ray diffraction; this allowed the delimitation of the vitreous zone. The inhibition of the mild steel corrosion in 1M HCl acid medium by this system was studied by polarization curve and electrochemical impedance spectroscopy. The obtained results showed a significant decrease in the corrosion current and an increase in charge transfer resistance when the compounds were added to the corrosive solution. This inhibition depends on the composition of the vitreous phase. The inhibitory efficiency reaches 79% at a concentration of 150 ppm for the S1 additive. The system acts primarily as a cathodic inhibitor by forming a stable film on the steel surface. The thermodynamic study showed that this film was formed by physisorption. Moreover, the inhibition efficiency increases with B_2O_3content, reaching a maximum value at 50% of B_2O_3 in our case is the inhibitor S5.

References

1- J. Zhang, J. Liu, W. Yu, Y. Yan, L. You, L. Liu, Corrosion. Sci., **2010**, 52, 2059-2065.
2- M. Iannuzzi, G.S. Frankel, Corrosion., **2007**, 63, 672-688.
3- A. Singh, S. K. Shukla, M. Singh, M. A. Quraishi, Mater. Chem. Phys., **2011,** 129, 68-76
4- S. K. Shukla, M. A.Quraishi, Mater.Chem.Phys., **2010**, 120, 142-147.
5- S. K. Shukla, A. K.Singh, I. Ahamad, M. A. Quraishi, Mater. Lett., **2009**, 63, 819-822.
6- S. K. Shukla, M. A. Quraishi, Corros. Sci., **2009**, 51, 1007-1011.
7- S. K. Shukla, M. A. Quraishi, R. Prakash, Corros. Sci., **2008**, 50, 2867-2872.
8- M. W. Ranney, Inhibitors Manufacture and Technology; **1976**, Noyes Data Corp: NJ,

9- F. Bentiss, M. Traisnel, H. Vezin, H.F. Hildebrand, M. Lagren, Corros.Sci., **2004**, 46, 2781-2792
10- R. A. Prabhu, T. V. Venkatesha, A. V. Shanbhag, B. M. Praveen, G. M. Kulkarni, R. G. Kalkhambkar, Mater. Chem. Phys., **2008**, 108, 283.
11- P. Lowmunkhong, D. Ungthararak, P. Sutthivaiyakit, Corros. Sci.,**2010**, 52, 30-36.
12- F. Bentiss, C. Jama, B. Mernari, H. E. Attari, L. E. Kadi, M. Lebrini, M. Traisnel, M. Lagrenee, Corros. Sci., **2009**, 51, 1628-1635.
13- M. R. Ali, C.M. Mustafa, M. Habib, J. Sci. Res., **2009,** 1, 82-91.
14- M. Iannuzzi, G.S. Frankel, Corrosion, **2007**, 63, 672-688.
15- G.H. Nancollas, Corrosion, **1983**, 39, 77-82.
16- G.H. Nancollas, Corrosion, **1983**, 39, 77-82.
17- M. Belfaquir, Guedira, S. D. Elyoubi, J.L. Rehspringer, Synthèse et caractérisation des phases du système ternaire Bi_2O_3- P_2O_5- B_2O_3, Ann. Chim. SciencesMatériaux , **2005**, 30, 27-35.
18- M. Belfaquir, T.Guedira, S. D. Elyoubi, J.L. Rehspringer, Etude structurale des verres borate du systèmeBi_2O_3- P_2O_5- B_2O_3, Sciences Lib Editions Mersenne, **2013**, 5.
19- M. Belfaquir, T. Guedira, S. D. Elyoubi, J.L. Rehspringer, Etude vibrationnelle et électrique des verres de phosphates isolés dans le système Bi_2O_3- P_2O_5- B_2O_3, Sciences Lib Editions Mersenne, **2013**, 5.
20- 20. B.B. Meera, A.K. Sppd, N. Chandradhas, J. Ramakrishna, Journal of Non-Crystalline Solids, **1990**, 12, 126, 224.
21- A. Pawlicka, M. Atik, M.A. Aegerter .Thin Solid Films, **1997**, 301, 236
22- T. Armaroli, G. Busca, C. Carlini, M. Giuttari, A.M.R. Galletti, G. Sbrana, *J. Mol. Catal.* A,**2000**, 151, 233.
23- M. Galai, J. choucri, Y. Hassani, H. Benqlilou, I. Mansouri, B. Ouaki, M. Ebn Touhami, C. Monticelli, F. Zucchi, Chemical Data Collections, **2019**, 19, 100171.
24- S.K. Shukla, M.A. Quraishi, Corros. Sci., **2009**, doi:10.1016/j.corros.2009.05.020.
25- M.G. Hosseini, M. Ehteshamzadeh, T. Shahrabi, Electrochem. Acta, **2007**, 52, 3680-3685
26- S. Murlidharan, K.L.N. Phani, S. Pitchumani, S. Ravichandran, J. Electrochem.Soc, **1995**, 142, 1478-1483
27- F. Bentiss, M. Traisnel, M. Lagrenee, Corros. Sci, **2000**, 42, 127-146.
28- B.G. Ateya, M.B.A. El-Khair, I.A. Abdel-Hamed, Corros. Sci, **1976**, 15, 163- 169
29- W. Li, Q. He, S. Zhang, C. Pei, B. Hou, J. Appl. Electrochem, **2008**,38, 289-295.
30- M. Galai, M. El Faydy, Y. El Kacimi, K. Dahmani, K. Alaoui, R. Touir, B. Lakhrissib and M. Ebn Touhami "Synthesis, Characterization and Anti-Corrosion Properties of Novel Quinolinol on C-steel in a Molar Hydrochloric Acid Solution." Portugaliae Electrochimica Acta, **2017**, 35(4), 233-251.
31- O.L. Riggs, Jr., Corrosion Inhibition, **1973**, second ed., C.C. Nathan, Houston, TX.
32- I. A. Ammar, F. M. El Khorafi, Werkst. Korros, **1973**, 24, 702.
33- K. Dahmani, M. Galai, M. Cherkaoui, A. El hasnaoui, A. El Hessni. J. Mater. Environ. Sci.**2017**, 8, 1676-1689.
34- A. Popova, E. Sokolova, S. Raicheva, M. Christov, AC and DC study of the temperature effect on mild steel corrosion in acid media in the presence of benzimidazole derivatives." Corrosion Science,**2003**, 45, 33-58.
35- T. Szauer, A. Brand, Adsorption of oleates of various amines on iron in acidic solution, Electrochim. Acta, **1981**, 26, 1253-1256.
36- H.Gerengi, K. Darowicki, G. Bereket, P. Slepski, Evaluation of corrosion inhibition of brass-118 in artificial seawater by benzotriazole using dynamic EIS, Corros. Sci, **2009**, 51, 2573-2579.
37- L. Saqalli, M. Galai, N. Gharda, M. Sahrane, R. Ghailane, M. Ebn Touhami, Y. Peres-lucchese, A. Souizi, N. Habbadi. Int. J. Electrochem. Sci., **2018**,13, 5096-5119.
38- A.K. Singh, S.K. Shukla, M. Singh, M.A. Quraishi, Inhibitive effect of ceftazidime on corrosion of mild steel in hydrochloric acid solution, Mater. Chem. Phys, **2011**,129,68-76.
39- M. Galai, M. Rbaa, Y. El Kacimi, M.Ouakki, N. Dkhirech, R. Touir, B. Lakhrissi and M. EbnTouhami, Anal. Bioanal. Electrochem, **2017**, 9, 80-101
40- A. Elbadaoui, M. Galai, M. Cherkaoui, T. Guedira. Preparation and characterization of a vitreous phase and application as a corrosion inhibitor in acidic medium. Der Pharma Chemica**, 2016**, 8, 214-221.
41- M. Galai, M. El Gouri, O. Dagdag, Y. El Kacimi, A. Elharfi, M. Ebn Touhami. New Hexa Propylene Glycol Cyclotiphosphazene As Efficient Organic Inhibitor of Carbon Steel Corrosion in Hydrochloric Acid Medium. J. Mater. Environ. Sci, **2016**, 7, 1562-1575.
42- A. Majjane, D. Rair, A. Chahine, M. Et-tabirou, M. Ebn Touhami, R. Touir, Preparation and characterization of a new glass system inhibitor for mild steel corrosion in hydrochloric solution. Corrosion Science, **2012**, 60, 98-103.